RSC Advances

PAPER

View Article Online
View Journal | View Issue

Cite this: *RSC Adv.*, 2023, **13**, 35592

The influence of UHMWPE with varying morphologies on the non-isothermal crystallization kinetics of HDPE

Hongwang Shen,[a] Yongxiang Hu,[a] Aiguo Gao,[c] Fantao Meng,[a] Lin Li*[b] and Guannan Ju*[a]

The current study aims to examine how the morphology of ultra-high molecular weight polyethylene (UHMWPE) particles impacts the kinetics of non-isothermal crystallization in high-density polyethylene (HDPE). To prepare blends of HDPE and UHMWPE, melt blending is utilized. High-temperature melting and subsequent shearing are used to cause the morphological changes in UHMWPE particles. The morphological evolution of UHMWPE particles is observed utilizing scanning electron microscopy (SEM). The non-isothermal crystallization kinetics of HDPE with varying UHMWPE morphologies are investigated using the Jeziony and Mo methods. The nucleation activity of UHMWPE particles in HDPE crystallization is assessed using the Dobreva and Gutzow model. Furthermore, the crystallization activation energy of HDPE blends is evaluated using the Friedman model. The results exhibit that after undergoing high-temperature melting, the UHMWPE particles underwent significant morphological changes, leading to enhanced interaction with the two phases and reduced nucleation activity. Additionally, it can increase the crystallization activation energy, which causes a decrease in the HDPE crystallization rate. However, subsequent shearing has crushed the UHMWPE particles into smaller pieces, enhancing their nucleation activity, decreasing the activation energy required for crystallization and increasing the HDPE crystallization rate.

Received 16th August 2023
Accepted 30th November 2023

DOI: 10.1039/d3ra05576k

rsc.li/rsc-advances

Introduction

High-density polyethylene (HDPE) has been widely utilized in various industries due to its exceptional performance, including its low cost, lightweight nature, excellent processibility, superior mechanical properties, and chemical stability.[1–4] With the continuous expansion of HDPE applications in injection molding, blow molding, and extrusion molding,[5,6] there has been a significant increase in the demand for its strength, toughness, stress-crack resistance, and wear resistance.[7–10] Several strategies have been designed to modify HDPE by introducing other polymers,[11,12] fibers,[8,13] and fillers,[14,15] which efficiently improves the comprehensive properties of HDPE.

It is well-known that the properties of polymer products largely depend on their microstructure (*e.g.* the crystallinity and crystalline morphology), which is primarily formed during processing stage. The crystallinity, crystalline morphology and crystallization rate of HDPE will significantly determine comprehensive properties, processability and mold processing productivity.[16–18] Moreover, the crystallization kinetics play a crucial role in governing the crystallization behavior. Hence, it is crucial to understand the polymer crystallization kinetics to optimize processing conditions and ensure product properties. Polymer crystallization can occur under either isothermal or non-isothermal conditions.[19] Isothermal crystallization kinetics are typically idealized and confined to a narrow temperature range.[18,20] However, the production process of crystalline polymers (*e.g.* HDPE) is dynamic and non-isothermal actual operation. Therefore, the kinetics of non-isothermal crystallization are more representative for actually industrial polymer processing and molding. The primary methods described the non-isothermal crystallization kinetics of semi-crystalline polymers (*e.g.* HDPE) include the Jeziorny method, Mo method and other similar methods.[21,22]

Numerous studies about the crystallization behavior of HDPE composites have been confirmed. Moreover, the polymer crystallization of HDPE is predominantly regulated by the nucleation stage.[19,23–25] To reduce the induction time and expedite the formation of crystalline nuclei, specific nucleation agents are often utilized to industrial polymer processing and molding. However, some commercial nucleation agents for HDPE have been limited, which maintains a challenge for the

[a]*School of Materials Science and Engineering, Shandong University of Technology, Zibo, Shandong 255000, China. E-mail: ju@sdut.edu.cn*

[b]*School of Materials Science and Engineering, National Institute for Advanced Materials, TKL of Metal and Molecule-Based Material Chemistry, Nankai University, Tianjin 300350, China. E-mail: lilin@nankai.edu.cn*

[c]*Shandong Hua Zhilin Pharmaceutical Co., Ltd, Zibo, Shandong 255000, China*

promotion of HDPE crystallization in academia and industry field.

Ultra-high molecular weight polyethylene (UHMWPE) exhibits similar molecular structure to HDPE. However, it possesses ultra-high molecular weight and viscosity, which results in superior toughness, stress crack resistance and wear resistance except poor processability. Numerous researchers have focused their efforts on the amalgamation of HDPE and UHMWPE to maximize the properties of HDPE. Liu *et al.*[26] induced the formation of more perfect crystals and higher crystallization degree of HDPE by melt blending 5 wt% UHMWPE. Diop *et al.*[27] prepared well-mixed UHMWPE/HDPE blends containing up to 50 wt% UHMWPE with excellent impact strength using solid-state shear pulverization melt extrusion. Therefore, HDPE is commonly used as a plasticizer and binder when blended with UHMWPE to improve its processability. Sui *et al.*[28] melt blended UHMWPE with 50 wt% HDPE to promote the flowability of UHMWPE melt. Yang *et al.*[29] blended UHMWPE with 5 wt% HDPE and successfully pelletized the blends with a standard twin-screw extruded with a tapered die. Some investigations have also delved into the crystallization behavior of HDPE/UHMWPE blends. For example, Song *et al.*[18] studied the isothermal crystallization kinetics of HDPE/UHMWPE blends, which discovered that a small quantity of UHMWPE could serve as a nucleation agent for the crystallization of HDPE, thereby accelerating its crystallization rates. Similarly, Shen *et al.*[30] observed that UHMWPE can increase the initial crystallization temperature of HDPE. Furthermore, oriented crystal structures of the shish-kebab structure can be induced by incorporating UHMWPE with HDPE under shear action.[31] However, UHMWPE particles dispersed in the HDPE matrix maintained their as-received morphology and poor compatibility due to its ultra-high molecular weight and high degree of molecular chain self-entanglement. As reported by Boscoletto *et al.*, no more than 3 wt% UHMWPE particles can be dissolved in the HDPE matrix, and only small amounts of UHMWPE can serve as tie molecules to improve interaction with HDPE.[32] If the UHMWPE could be more effectively dispersed in HDPE with an optimized morphology and improved compatibility, it would likely result in even better performance. Therefore, the influence of morphological evolution of UHMWPE on the crystallization behavior of HDPE is still vague. Moreover, there have been few relevant experimental reports that are relevant to alter the UHMWPE morphology within the HDPE matrix.

In this paper, a small amount of UHMWPE particle is introduced into HDPE matrix through melt blending, followed by a treatment involving high-temperature melting and subsequent shearing to alter the morphology of UHMWPE particles. The objective of our work is to conform the effect of the UHMWPE morphological evolution on the HDPE crystallization. Furthermore, differential scanning calorimetry (DSC) is used to investigate the non-isothermal crystallization behaviors of HDPE/UHMWPE blends. The kinetics data are subjected to analysis using the Jeziony and Mo methods. Importantly, the crystallization activation energy and nucleation activity are also calculated, which provides theoretical guidance for improving the comprehensive properties of composite.

Results and discussion

Morphological characterization

Fig. 1 shows SEM micrographs of various blends of HDPE and UHMWPE. As depicted in Fig. 1a, sample H/U exhibits characteristic "sea–island" structures, wherein UHMWPE particles measuring around 100 μm disperse in the HDPE matrix, and a distinct phase interface between HDPE and UHMWPE is noticeable. This finding is consistent with previous studies.[28,29,32] The main reason for this issue is the extremely slow diffusion of UHMWPE molecular chains. According to the reptation theory of de Gennes[33] and the tube model of Edwards,[34] the terminal relaxation time for a UHMWPE molecular chain (weighing about 10^6 g mol^{-1}) is approximately 15 hours at 180 °C.[35] This time frame is much longer than the melt blending time. Therefore, UHMWPE molecular chains do not have sufficient time to diffuse across the phase interface and establish adequate entanglement between HDPE and UHMWPE under ordinary melt blending conditions in this study.

After high-temperature melting, the phase interface becomes ambiguous, and the size of UHMWPE particles increases with increasing melting duration (see Fig. 1b and c). This is mainly due to chain inter-diffusion between HDPE and UHMWPE,

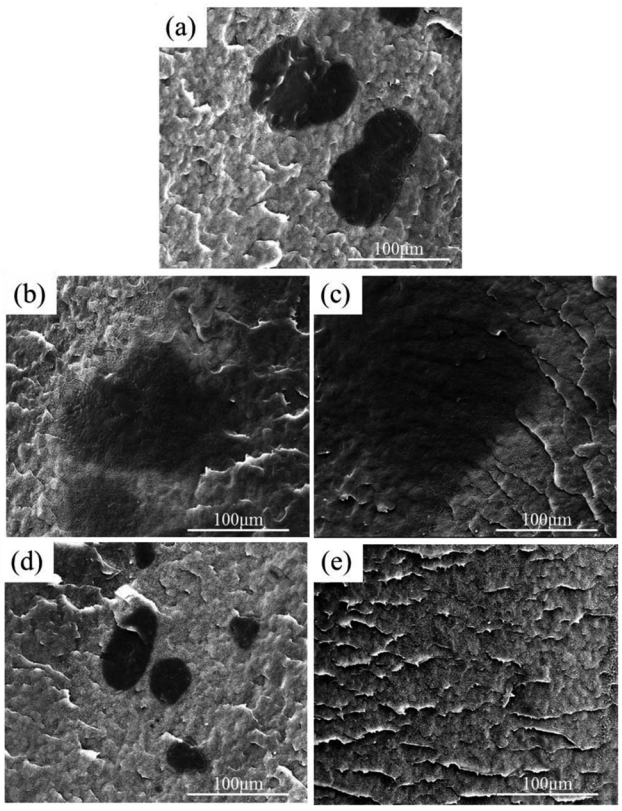

Fig. 1 SEM micrographs of samples: (a) H/U, (b) H/U_2, (c) H/U_{10}, (d) H/U_2-S and (e) H/U_{10}-S.

which is caused by high-temperature melting. And an adequate entanglement between HDPE and UHMWPE can be established during high-temperature melting. It can be understood that the UHMWPE particles are partially or entirely swollen by HDPE chains, and the degree of swelling increases with longer melting duration. Whereafter, the swollen UHMWPE particles can be broken up during subsequent shear because of significant reduction of UHMWPE chains entanglement, resulting in better dispersion with smaller sizes (as shown in Fig. 1d) and even becoming invisible (as shown in Fig. 1e). Additionally, new and distinct interfaces appear between the remaining non-swollen portion of UHMWPE particles and HDPE. Hence, high-temperature melting and subsequent shear have played an effective role in bringing about the morphological evolution of UHMWPE particles in HDPE.

Non-isothermal crystallization behavior

Fig. 2 depicts the non-isothermal crystallization curves of various samples experiencing different cooling rates. By analyzing the DSC curves, we can obtain several parameters, including the crystallization onset temperature (T_o), the crystallization peak temperature (T_p), the crystallization ending temperature (T_e), and the enthalpy of fusion (ΔH_m). The corresponding values for these parameters are listed in Table 1.

Compared with sample H/U, the high-temperature melting leads to a reduction in T_o, T_p, and T_e values of sample H/U_t at the same cooling rate, indicating the overall crystallization becomes slower after high-temperature melting. Moreover, increasing the melting duration has no impact on the T_o value of sample H/U_t, while slightly decreasing the T_p and T_e values, inferring that the swelling degree of UHMWPE particle mainly affects the crystal growth stage rather than the nucleation during crystallization. Besides, the high temperature melting slightly increases ΔH_m, indicating a higher degree of crystallinity. This is contributed to the border crystallization temperature range, certified by an increase in the value of $T_o - T_e$ with an increase in the melting duration.

Significantly, the subsequent shear shifts the values of T_o and T_p to a higher temperature (*e.g.* 121.8 °C and 120.4 °C of H/U_{10}-S from 120.5 °C and 119.3 °C of H/U), and increase the ΔH_m values (*e.g.* 181.5 J g^{-1} of H/U_{10}-S from 173.5 J g^{-1} of H/U), even higher than that of sample H/U, indicating promotion for the crystallization and increase in the crystallinity of blends. The main reason is the better dispersion of UHMWPE particles in HDPE, which may play a more effective nucleation act for the crystallization of HDPE. Summarily, the morphological evolution of UHMWPE caused by high-temperature melting or subsequent shear has negative or positive effects on the crystallization behavior of HDPE.

The relationship between relative crystallinity (X_t) and time (t) are shown in Fig. 3. It can be seen that sample H/U_t shows the longest crystallization time at the early stage of crystallization, while sample H/U_t-S has the shortest crystallization time, especially at the lower cooling rate. This is consistent with the variation trend of T_o in Table 1. It is well known that at a higher temperature (early stage of crystallization), the formation rate of nuclei is lower than the growth rate of crystals and the overall crystallization rate of polymer is mainly determined by the nucleation rate. Consequently, we may conclude that the swollen UHMWPE particles after high-temperature melting (in H/U_t) have a weaker nucleation efficiency on the crystallization of HDPE than the as-receive UHMWPE particles in H/U, while better dispersion of UHMWPE after subsequent shear (in H/U_t-S) is likely to induce efficiently the formation of more nuclei which leads to an increase of overall crystallization rate.

In addition, the half time of crystallization ($t_{1/2}$, the time when relative crystallinity is 50%) are listed in Table 1. At the same cooling rate (*e.g.* 2.5 °C min^{-1}), the $t_{1/2}$ value of H/U_t (1.774 min) is larger than that of sample H/U (1.597 min), and it increases with an increase in the melting duration. This is an indication that the high-temperature melting decelerates the crystallization of HDPE. The weaker nucleation of swollen UHMWPE particles mentioned above is the main reason. It is worth noting that the $t_{1/2}$ value of H/U_t-S (1.474 and 1.564 min) is significantly lower than that of H/U (1.597 min), indicating a significant acceleration effect on the crystallization rate after subsequent shear. And H/U_2-S has the lowest $t_{1/2}$ values, it is mainly attributed to the increase in the melt viscosity of the system with increasing the melting duration. In the previous works, it has been proved that the melt viscosity of samples H/U_t-S increased by about 67% by extending the melting duration from 2 h to 10 h.[30] A high melt viscosity can hinder the molecular chain movement, reducing the crystallization rate.

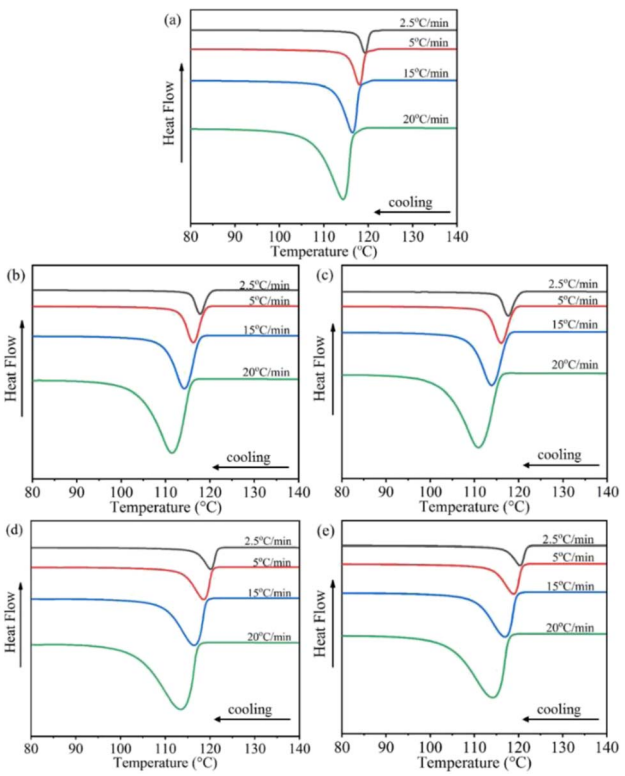

Fig. 2 DSC curves of non-isothermal crystallization of samples at different cooling rates: (a) H/U, (b) H/U_2, (c) H/U_{10}, (d) H/U_2-S, (e) H.

Table 1 Non-isothermal crystallization parameters of blends

Samples	φ (°C min^{-1})	T_o (°C)	T_p (°C)	T_e (°C)	ΔH_m (J g^{-1})	$t_{1/2}$ (min)	n
H/U	2.5	120.5	119.3	117.5	173.5	1.597	2.91
	5	119.4	118.0	115.5	170.3	0.902	
	10	118.1	116.4	112.3	171.8	0.571	
	20	116.4	114.4	107.8	168.7	0.334	
H/U$_2$	2.5	119.8	117.8	115.7	178.2	1.766	2.85
	5	118.8	116.3	113.3	175.2	0.918	
	10	117.5	114.2	109.7	171.8	0.605	
	20	115.7	111.5	104.3	168.7	0.362	
H/U$_{10}$	2.5	119.8	117.6	115.4	179.5	1.774	2.84
	5	118.8	116.1	112.9	176.1	1.087	
	10	117.5	113.9	109.2	173.0	0.611	
	20	115.7	111.0	103.2	170.1	0.373	
H/U$_2$-S	2.5	121.6	120.1	116.6	181.1	1.474	2.96
	5	120.5	118.6	113.3	177.9	0.834	
	10	119.1	116.5	109.8	174.3	0.507	
	20	117.2	113.5	103.4	171.4	0.294	
H/U$_{10}$-S	2.5	121.8	120.4	116.6	181.5	1.564	3.01
	5	120.8	118.9	114.0	177.9	0.864	
	10	119.5	117.0	110.2	174.8	0.520	
	20	117.7	114.1	104.1	171.8	0.313	

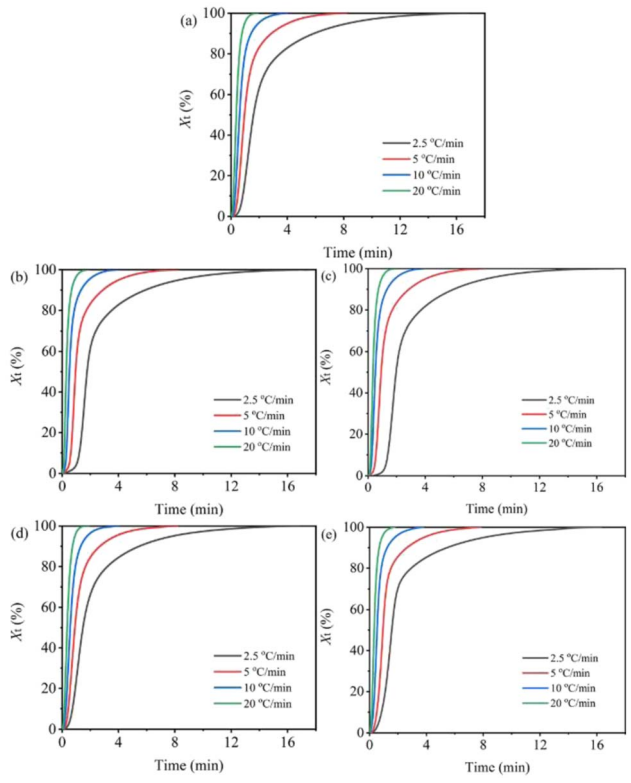

Fig. 3 Relative degree of crystallinity *versus* time for non-isothermal crystallization of samples at different cooling rates: (a) H/U, (b) H/U$_2$, (c) H/U$_{10}$, (d) H/U$_2$-S, (e) H/U$_{10}$-S.

Non-isothermal crystallization kinetics analyses

Analysis based on the Avrami theory modified by Jeizorny method. The Avrami equation has been used widely to describe isothermal crystallization kinetics of semi-crystalline polymers, it is expressed as:[36]

$$1 - X_t = \exp(-Z_t t^n) \quad (1)$$

$$\lg[-\ln(1 - X_t)] = \lg Z_t + n \lg t \quad (2)$$

where X_t is the relative crystallinity at an arbitrary time t, n is the Avrami exponent depending on the nucleation mechanism and the geometry of crystal growth, and Z_t is the crystallization rate constant.

Jeziorny modified the crystallization rate constant Z_t in the Avrami equation by dividing by the cooling rate φ to eliminate the influence of the cooling rate during the non-isothermal crystallization process, as follows:[21]

$$\lg Z_c = \lg Z_t/\varphi \quad (3)$$

where Z_c is the non-isothermal crystallization rate constant.

The curves of $\lg[-\ln(1 - X_t)]$ *versus* $\lg t$ for samples at different φ are presented in Fig. 4. The upper limit about 65% for the relative crystallinity in linear regression was chosen to investigate the primary crystallization, and a good linear relationship is obtained. Therefore, the values of Z_c and n can be obtained from the slope and the intercept of the fitted straight line.

Fig. 5 illustrates the changes in the Z_c value of blends after the high-temperature melting and subsequent shear. The larger values of Z_c represent faster crystallization rates. As can be seen, the Z_c value of all samples increases with an increase in the cooling rate. At an equivalent cooling rate (*e.g.* 2.5 °C min^{-1}), the high-temperature melting decreases the Z_c value to 0.436 of H/U$_{10}$ from 0.496 of H/U, while the subsequent shear brings an apparent increase in the Z_c values (*e.g.* 0.571 of H/U$_2$-S). This

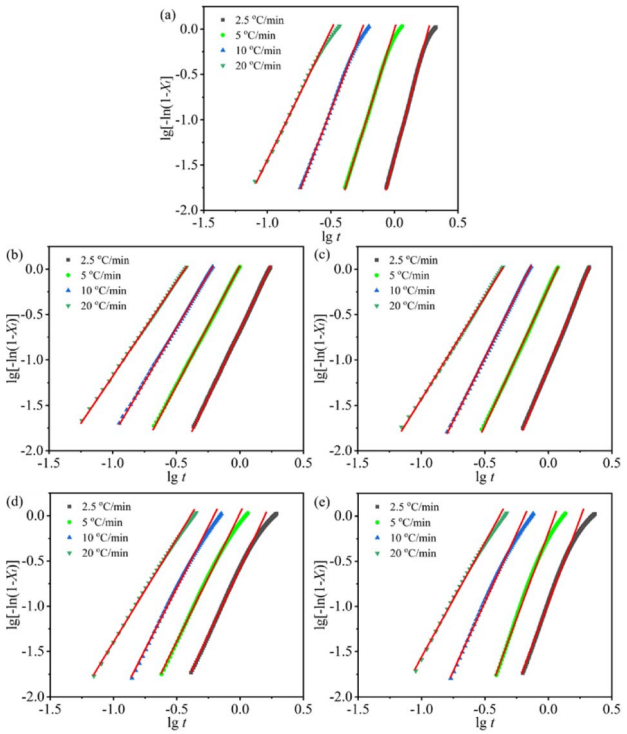

Fig. 4 The lg[−ln(1 − X_t)] *vs.* lg t curves of samples at different cooling rates: (a) H/U, (b) H/U_2, (c) H/U_{10}, (d) H/U_2-S and (e) H/U_{10}-S.

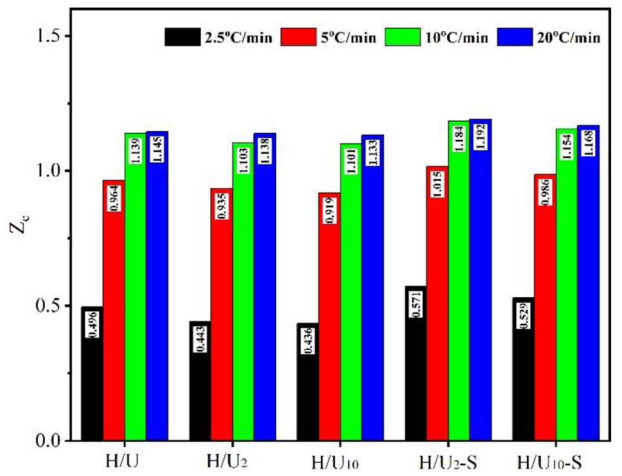

Fig. 5 Dependence of the Z_c on the HMT duration for all samples.

indicates that the high-temperature melting plays a negative role in the crystallization rate due to the suppression of nucleation, while the subsequent shear improves the crystallization rate because of enhancement in nucleation. Meanwhile, expanding melting duration brings up a slight decline in the Z_c value (*e.g.* 0.571 of H/U_2-S to 0.529 of H/U_{10}-S) owing to high melt viscosity reducing the mobility of the molecular chain. All these are a result of the morphological evolution of UHMWPE particles in the HDPE matrix. These results are in good agreement with the conclusion from DSC data in Table 1.

Due to the crystallization occurring under non-isothermal condition, the analysis of Avrami exponent n become complicated in contrast with isothermal crystallization, and it does not have the same physical meaning as under isothermal conditions. Hence, Harnisch and Muschik suggested that the Avrami index under non-isothermal conditions can be expressed by the following equation:[37]

$$n = 1 + \frac{\{\ln[\Phi_{t,1}/(1 - X_{t,1})] - \ln[\Phi_{t,2}/(1 - X_{t,2})]\}}{\ln(\varphi_2/\varphi_1)} \quad (4)$$

where X_t is the relative crystallinity, calculated from the DSC data, Φ_t is the derivative of the relative crystallinity and φ is the cooling rate. The index n is calculated at a certain temperature in the crystallization range by inserting the crystallinity values and the derivatives obtained at two different cooling rates 1 and 2 into eqn (6). Parallel straight lines can be obtained by plotting $\ln[\Phi_t/(1 - X_t)]$ *vs.* T at different cooling rates, the value of $\ln[\Phi_{t,1}/(1 - X_{t,1})] - \ln[\Phi_{t,2}/(1 - X_{t,2})]$ is then obtained as the vertical distance between two of these parallel lines. The n values of samples calculated according to eqn (6) are listed in Table 1. The n values of all samples are around 3 were obtained, and the n value of H/U_t slightly decreases, while that of H/U_t-S slightly increases in comparison with H/U. Some workers also obtained similar results when they blended nucleation agents with HDPE.[18,38] Therefore, the morphological evolution of UHMWPE particles may change the nucleation type and geometry of the crystal growth of HDPE.

Mo method. Mo method proposed another efficient approach to describe the non-isothermal crystallization process by combining the Avrami and Ozawa equations as follows:[22]

$$\lg \varphi = \lg F(T) - \alpha \lg t \quad (5)$$

$$F(T) = [K(T)/Z_t]^{1/m} \quad (6)$$

$$\alpha = n/m \quad (7)$$

where $K(T)$ and m are the kinetic parameters from Ozawa equation.[39] The physical mean of parameter $F(T)$ is the necessary cooling rate when the measured system reaches a certain degree of crystallinity at unit crystallization time and a lower value of $F(T)$ means a higher crystallization rate. According to eqn (7), plotting lg φ *versus* lg t at a given degree of crystallinity is shown in Fig. 6, and a strong linear relationship is present for all samples. The kinetic parameters $F(T)$ and α can be determined by the intercept and slope of the fitted straight lines, and are listed in Table 2.

As can be seen from Table 2, the value of $F(T)$ of samples H/U_t is higher than that of sample H/U and the longer duration causes more difference, indicating that the high-temperature melting decelerates the crystallization rate. It is worth noting that subsequent shear significantly reduces the value of $F(T)$ as compared to sample H/U, the sample H/U_2-S shows the lowest $F(T)$ values (1.706–4.394 at X_t = 10–50%) and the fastest crystallization rate. However, the values of $F(T)$ (5.472–13.90) are higher than that of H/U (5.107–12.91) and H/U_t (5.409–13.44) at higher relative crystallinity (X_t > 60%). It is mainly due to the

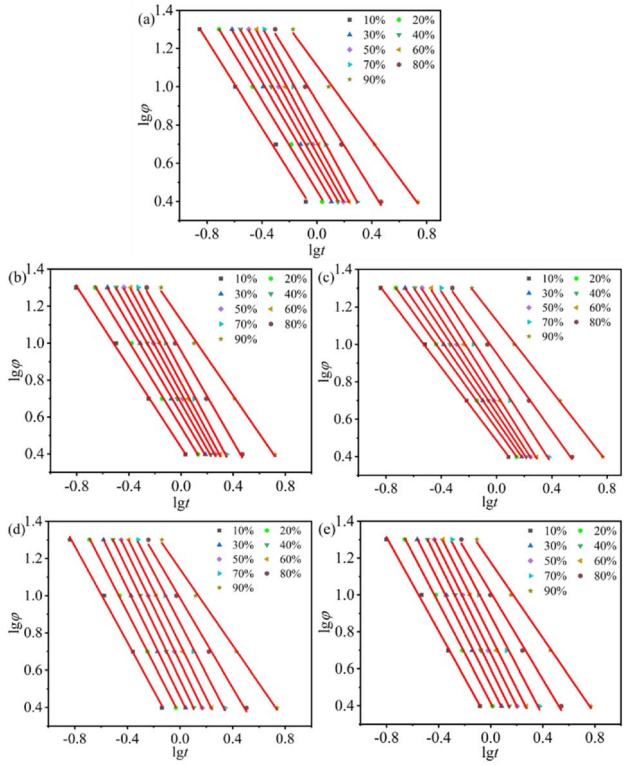

Fig. 6 The lg φ *vs.* lg t curves of non-isothermal crystallization for all samples at different cooling rates: (a) H/U, (b) H/U_2, (c) H/U_{10}, (d) H/U_2-S and (e) H/U_{10}-S.

obvious enhancement of the melting viscosity, which reduces the crystallization rate because of hindering the movement of molecular chains. This is also the reason that the value of $F(T)$ of H/U_{10}-S is higher than that of H/U_2-S. Therefore, it can be concluded that the cooperation between the high temperature melting and subsequent shear significantly improves the crystallization rate. These results agree with the conclusion based on the Z_c value using Jeziorny model and half-crystallization time $t_{1/2}$, as previously described.

Nucleation activity. In order to evaluate the effects of UHMWPE particles as a nucleation agent for the crystallization of HDPE, the nucleating activity (ϕ) is determined by the Dobreva and Gutzow method as follows:[40]

$$\ln \varphi = C - B/\Delta T^2 \quad (8)$$

where φ is the cooling rate, C is a constant and ΔT is the supercooling ($T_m - T_p$). B and B^* are the parameters of homogeneous and heterogeneous medium for HDPE, respectively. As shown in Fig. 7a, straight lines can be obtained by plotting ln φ *versus* $1/(\Delta T)^2$, and the value of B and B^* can be calculated from the slopes of the fitted lines. The nucleating activity $\phi = B^*/B$ is presented in Fig. 7b, and if the UHMWPE particle does not act as a nucleation agent, the value of ϕ will be 1, while it is more conducive to activation nucleation, ϕ approaches 0. As can be seen from Fig. 7b, the high-temperature melting causes a higher ϕ value (0.79 of H/U_{10}) as compared to H/U (0.67), indicating a lower nucleation efficiency. Significantly, subsequent shear enhances the nucleation activity and the better efficiency is the longer the duration is, sample H/U_{10}-S shows the best nucleation activity with the lowest ϕ value of 0.56. It may be attributed to the formation more nucleation sites caused by UHMWPE particles being broken into small ones after subsequent shear.

Crystallization activation energy. The isoconversional method of Friedman was used to determine the activation energy of non-isothermal crystallization[41] through the following equation:

$$\ln\left(\frac{dX_t}{dt}\right)_{X_t,\varphi} = \ln[Af(X_t)] - \left(\frac{\Delta E_X}{RT_{X_t,\varphi}}\right) \quad (9)$$

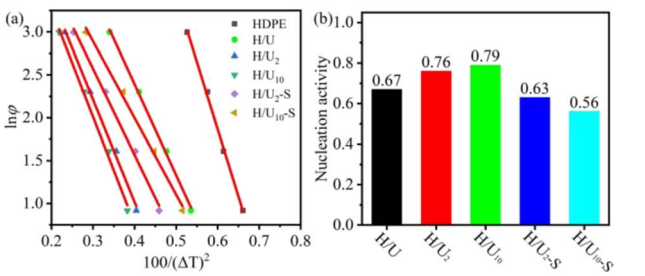

Fig. 7 Plots of ln φ *versus* $1/(\Delta T)^2$ (a) and nucleation activity (b) obtained from Dobreva–Gutzow model of all samples.

Table 2 Mo parameters of non-isothermal crystallization kinetics for all samples

		X_t (%)								
Samples	Parameters	10	20	30	40	50	60	70	80	90
H/U	$F(T)$	2.116	2.858	3.426	3.939	4.478	5.107	6.093	8.393	12.91
	α	1.151	1.228	1.279	1.302	1.319	1.304	1.239	1.117	0.986
H/U_2	$F(T)$	2.731	3.510	3.914	4.303	4.760	5.409	6.641	8.953	13.44
	α	1.089	1.158	1.210	1.251	1.290	1.318	1.334	1.231	1.026
H/U_{10}	$F(T)$	3.060	3.540	4.146	4.734	5.367	6.088	7.085	9.082	13.35
	α	0.978	1.034	1.097	1.116	1.146	1.181	1.153	1.036	0.948
H/U_2-S	$F(T)$	1.706	2.281	2.860	3.542	4.394	5.472	7.115	9.713	13.90
	α	1.293	1.380	1.452	1.477	1.469	1.437	1.367	1.205	1.023
H/U_{10}-S	$F(T)$	1.975	2.600	3.239	3.970	4.825	5.945	7.678	10.317	15.04
	α	1.276	1.353	1.406	1.447	1.430	1.413	1.346	1.177	1.026

where A is a preexponential factor, $f(X_t)$ is the crystallization model, and can be considered as constant at a certain X_t. Values of dX_t/dt are the instantaneous crystallization rate for a certain relative crystallinity and can be calculated through non-isothermal crystallization experiments with different cooling rates. ΔE_X is the effective activation energy of the crystallization process at a given X_t, R is the universal gas constant (8.314 J (mol K)$^{-1}$), and T is the set of temperatures related to a certain X_t at different cooling rates φ. Plotting $\ln(dX_t/dt)$ *versus* $1/T$ at different degrees of crystallization with various cooling rates results in straight lines (as shown in Fig. 8), and ΔE_X can be calculated from the slop of lines at a certain cooling rate and relative crystallinity, are listed in Table 3.

Fig. 8 shows the Friedman plots for samples at different relative crystallinity. ΔE is the sum of the activation energy of the nucleation and crystal growth processes, and a lower ΔE represents the crystallization is easier. It can be seen that the absolute value of ΔE for each sample first decreases and then increases with an increase in relative crystallinity. At a given relative crystallinity (*e.g.* 10%), the absolute value of ΔE for samples H/U$_t$ (366.5, 392.3) is larger than that of sample H/U (348.5), and the value increases with the increase in the melting duration, indicating the crystallization of HDPE becomes more difficult after the high-temperature melting. It is chiefly because the UHMWPE particles are swollen after high-temperature melting, which weakens the nucleating efficiency

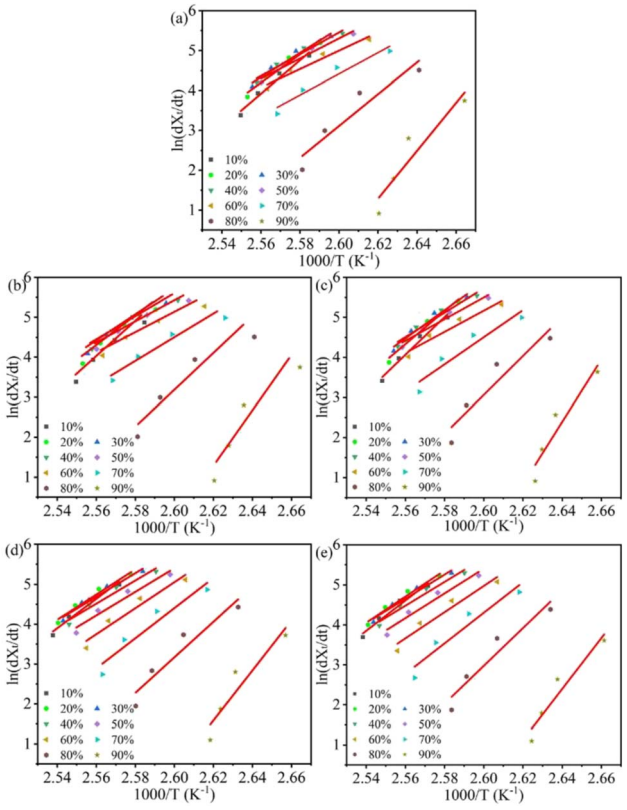

Fig. 8 Plots of $\ln(dX_t/dt)$ *versus* $1/T$ for non-isothermal crystallization of all samples: (a) H/U, (b) H/U$_2$, (c) H/U$_{10}$, (d) H/U$_2$-S and (e) H/U$_{10}$-S.

Table 3 Non-isothermal crystallization activation energy by Friedman method

	ΔE/kJ mol^{-1}				
X_t/%	H/U	H/U$_2$	H/U$_{10}$	H/U$_2$-S	H/U$_{10}$-S
10	−348.5	−366.5	−392.3	−306.8	−316.1
20	−294.9	−309.9	−344.5	−263.2	−272.1
30	−264.6	−270.6	−292.8	−247.4	−252.8
40	−248.1	−250.9	−253.9	−241.8	−248.2
50	−218.9	−219.9	−225.1	−246.5	−257.5
60	−215.1	−217.1	−219.5	−271.4	−272.7
70	−240.6	−245.9	−281.3	−314.3	−318.1
80	−331.4	−383.1	−404.3	−434.9	−452.9
90	−559.9	−576.3	−572.5	−621.7	−629.8

on the crystallization of HDPE, resulting in a higher energy barrier of crystal nucleation.

Notably, the absolute value of ΔE at lower relative crystallinity significantly decreases after subsequent shear. By contrast, the values are larger than that of samples H/U and H/U$_t$ at higher relative crystallinity. For example, the absolute value of ΔE for H/U$_2$-S at $X_t = 10\%$ decreases by approximately 11% compared to that of H/U, but it increases by about 12% at $X_t = 50\%$. This can be attributed to better dispersion of UHMWPE particles. On the one hand, the formation of a great many small particles induces to form more nuclei sites, which is conducive to nucleation and declines the activation energy; on the other hand, increasing the quantity of spherulite aggravate squeeze each other at higher X_t, impeding the crystal growth and increasing the activation energy. Besides, the higher melt viscosity of sample H/U$_t$-S hinders the movement of molecular chains and is also a reason for the increase in the activation energy. These results are consistent with the trends seen in the calculation of non-isothermal crystallization kinetics analysis.

Experiments

Materials

HDPE pellet (trade name 5000S) with weight averaged molecular mass (M_w) of 3.73×10^5 g mol^{-1}, molecular weight distribution (M_w/M_n) of 4.3 and the melt flow index (MFI) of 1.18 g/10 min (190 °C, 2.16 kg), was purchased from Lanzhou Petro-Chemical Co. Ltd (China). UHMWPE powder (trade name M-II) with $M_w = 2.5 \times 10^6$ g mol^{-1} was purchased from Beijing second auxiliary agent factory (China). Antioxidant (Irganox 1010) was purchased from BASF Co. Ltd (Germany).

Sample preparation

HDPE was blended with UHMWPE in an internal mixer (XSS-300, Shanghai Kechuang Rubber Plastic Mechanical Equipment Co., Ltd, China) with a rotor speed of 60 rpm at 180 °C. HDPE was first melted and then UHMWPE powder was added after 2 min, the melt blending continued for about 10 min until the torque is balanced. The content of UHMWPE in the blends was set as 7 wt%. In order to prevent degradation, 0.5 wt% of antioxidants (1010) to the total weight of the blend was used

during mixing. This HDPE/UHMWPE blend was denoted as H/U.

High-temperature melting and subsequent shear treatment

High-temperature melting treatment of HDPE/UHMWPE blends was carried out in a programmable oven under a purity dry nitrogen atmosphere. The oven was pre-heated to a preset temperature with a nitrogen purge, then HDPE/UHMWPE blend was placed in the oven and purged again. The sample was held at 280 °C for 2 h or 10 h under continuous nitrogen flow, and then naturally cooled down to 40 °C in the oven before retrieval. Such melted HDPE/UHMWPE was denoted as H/U_t, where t is the melting duration. Specifically, sample H/U_2 represents HDPE/UHMWPE melted at 280 °C for 2 h. Afterward, the high-temperature melted samples were exposed to shear in the internal mixer with a rotor speed of 60 rpm at 180 °C for 5 min, and such samples were denoted as H/U_t-S. For example, sample H/U_2-S represents HDPE/UHMWPE blend was firstly melted at 280 °C for 2 h and followed by subsequent shear.

Characterizations

Scanning electron microscopy (SEM). The morphology analysis was conducted on the cryogenically fractured surface of samples using scanning electron microscopy (SEM, model 450, FEI Company, USA) with a 20 kV accelerating voltage. The samples were pre-cracked with a razor blade and immersed in liquid nitrogen for 30 min before they were fractured, and the observing surfaces were gold sputtered before SEM observation.

Differential scanning calorimetry (DSC) measurements. The non-isothermal crystallization behavior of HDPE/UHMWPE blends was carried out using a differential scanning calorimeter (Q2000, TA Instruments Co., USA) under a nitrogen atmosphere. About 10 mg samples were sealed into aluminum pans and first heated to 160 °C at 10 °C min^{-1}, kept at this temperature for 5 min to remove any previous thermal history. Then samples were cooled to 40 °C at different constant cooling rates (φ) (φ = 2.5, 5, 10 and 20 °C min^{-1}). Finally, samples were heated again to 160 °C at 10 °C min^{-1}. The exothermic and endothermic curves were recorded, and the exothermic curves were taken for kinetic analysis. In order to ensure the reliability of the measurement results, all the specimens were measured three times.

Conclusions

In this paper, we described the morphological evolution of UHMWPE particles dispersed in the HDPE matrix. The non-isothermal crystallization kinetics of HDPE/UHMWPE blends as a function of this evolution using Jeziony and Mo methods was investigated. Additionally, we calculated the crystallization activation energy and nucleation activity using the Friedman method and Dobreva–Gutzow method, respectively. The HDPE/UHMWPE blends were prepared by melt blending, and the high-temperature melting and subsequent shear significantly changed the particle morphology of UHMWPE, leading to an enhancement of interaction between the two phases and the formation of small UHMWPE particles. Based on these morphological changes, the high-temperature melting decelerated the crystallization rate of HDPE due to the weakening of the nucleation efficiency of UHMWPE particles for HDPE crystallization. The longer the duration, the more obvious this effect became. However, the subsequent shear resulted in an acceleration of the crystallization rate due to the enhancement of nucleation efficiency. The nucleation activity was calculated to confirm these observations, revealing that the order of nucleation activity from highest to lowest was H/U_{10}-S, H/U_2-S, H/U, H/U_2, and H/U_{10}. Additionally, the absolute crystallization activation energy showed an increase after high-temperature melting but a decrease after subsequent shear. Sample H/U_2-S had the lowest activation energy compared to the other samples. Therefore, it can be concluded that the evolution of UHMWPE morphology has a significant impact on the non-isothermal crystallization process of HDPE. H/U_2-S was determined to be an ideal sample for enhancing the crystallization rate and reducing the crystallization activation energy for HDPE/UHMWPE blends.

Author contributions

H. S. designed the research. H. S., X. H. and F. M. carried out the analytical and numerical calculations. The manuscript was written by G. J., H. S., and L. L.

Conflicts of interest

The authors declare no competing financial interest.

Acknowledgements

This work was supported by the Natural Science Foundation of Shandong Province (Grants ZR2023ME233); the Innovation Ability Improvement Project of Science and Technology SMEs in Shandong Province (Grants 2022TSGC1166); China Postdoctoral Science Foundation (2022TQ0162).

Notes and references

1 L. Zhang, C. Lu, P. Dong, K. Wang and Q. Zhang, Realizing mechanically reinforced all-polyethylene material by dispersing UHMWPE via high-speed shear extrusion, *Polymer*, 2019, **180**, 121711.
2 C. Zhu, Y. Zhang, X. Zhou, F. Kong and G. Jiang, Influence of the amphiphilic molecule on high-density polyethylene crystallization, *J. Therm. Anal. Calorim.*, 2021, **147**, 4151.
3 S. Tesfaw, T. M. Bogale and O. Fatoba, Evaluation of tensile and flexural strength properties of virgin and recycled high-density polyethylene (HDPE) for pipe fitting application, *Mater. Today: Proc.*, 2022, **62**, 3103.
4 F. M. Salleh, A. Hassan, R. Yahya and A. D. Azzahari, Effects of extrusion temperature on the rheological, dynamic mechanical and tensile properties of kenaf fiber/HDPE composites, *Composites, Part B*, 2014, **58**, 259.

5 Y. Xiang, Z. Hou, R. Su, K. Wang and Q. Fu, The effect of shear on mechanical properties and orientation of HDPE/mica composites obtained via dynamic packing injection molding (DPIM), *Polym. Adv. Technol.*, 2010, **21**, 48.

6 A.-M. Yousefi, J. den Doelder, M.-A. Rainville and K. A. Koppi, A modeling approach to the effect of resin characteristics on parison formation in extrusion blow molding, *Polym. Eng. Sci.*, 2009, **49**, 251.

7 M. Amjadi and A. Fatemi, Creep behavior and modeling of high-density polyethylene (HDPE), *Polym. Test.*, 2021, **94**, 107031.

8 T. A. Negawo, Y. Polat and A. Kilic, Effect of compatibilizer and fiber loading on ensete fiber-reinforced HDPE green composites: Physical, mechanical, and morphological properties, *Compos. Sci. Technol.*, 2021, **213**, 108937.

9 B. D. Rao, A. Pradhan and K. K. Sethi, Study of wear performance and mechanical properties of HDPE on addition of CNT fillers, *Mater. Today: Proc.*, 2022, **62**, 7501.

10 B. Suresha, Sriraksha and R. Hemanth, Mechanical Performance of HDPE/UHMWPE Hybrid Composites and Tribological Characterization using Taguchi Method, *Mater. Today: Proc.*, 2020, **24**, 1452.

11 Y. Chen, X. Nie, S. Zhou, H. Zou, M. Liang and P. Liu, Investigations of environmental stress cracking resistance of HDPE/UHMWPE and LDPE/UHMWPE blends, *J. Polym. Res.*, 2013, **20**, 140.

12 G. Savini and R. L. Oréfice, Toughening high density polyethylene submitted to extreme ambient temperatures, *J. Polym. Res.*, 2017, **24**, 78.

13 M. Fatima Ezzahrae, A. Nacer, E. Latifa, Z. Abdellah, I. Mohamed and J. Mustapha, Thermal and mechanical properties of a high-density polyethylene (HDPE) composite reinforced with wood flour, *Mater. Today: Proc.*, 2023, **72**, 3602.

14 V. Balobanov, T. Verho, V. Heino, H. Ronkainen and J. Pelto, Micromechanical performance of high-density polyethylene: Experimental and modeling approaches for HDPE and its alumina-nanocomposites, *Polym. Test.*, 2021, **93**, 106936.

15 A. Samadam, R. Vallepalli, K. Neeraj Kumar, M. Sreekanth and R. Raman Goud, Mechanical properties evaluation and behaviour of cellulose-HDPE composite, *Mater. Today: Proc.*, 2022, **62**, 3405.

16 L. Amoroso, E. L. Heeley, S. N. Ramadas and T. McNally, Crystallisation behaviour of composites of HDPE and MWCNTs: The effect of nanotube dispersion, orientation and polymer deformation, *Polymer*, 2020, **201**, 122587.

17 W. Shao, L. Liu, Y. Wang, X. Hua, F. Zhang and Y. Shi, Crystallization, structure, and properties of polypropylene random copolymer (PPR)/high-density polyethylene/polypropylene grafted maleic anhydride ((HDPE/PP)-g-MAH) blends, *J. Polym. Res.*, 2022, **29**, 353.

18 S. Song, P. Wu, M. Ye, J. Feng and Y. Yang, Effect of small amount of ultra high molecular weight component on the crystallization behaviors of bimodal high density polyethylene, *Polymer*, 2008, **49**, 2964.

19 A. Z. A. Abuibaid and M. Z. Iqbal, Thermally reduced graphene/polyethylene nanocomposites: effects of graphene on isothermal and nonisothermal crystallization of polyethylene, *Heliyon*, 2020, **6**, e03589.

20 X. Fu, X. Dong, G. Yang and S. Bai, Non-isothermal crystallization kinetics of graphene/PA10T composites, *Heliyon*, 2020, **8**, e10206.

21 A. Jeziorny, Parameters characterizing the kinetics of the non-isothermal crystallization of poly(ethylene terephthalate) determined by d.s.c, *Polymer*, 1978, **19**, 1142.

22 T. Liu, Z. Mo, S. Wang and H. Zhang, Nonisothermal melt and cold crystallization kinetics of poly(aryl ether ether ketone ketone), *Polym. Eng. Sci.*, 1997, **37**, 568.

23 H. J. Kim, J. J. Lee, J.-C. Kim and Y. C. Kim, Effect of starch content on the non-isothermal crystallization behavior of HDPE/silicate nanocomposites, *J. Ind. Eng. Chem.*, 2010, **16**, 406.

24 S. Coba-Daza, E. Carmeli, I. Otaegi, N. Aranburu, G. Guerrica-Echevarria, S. Kahlen, D. Cavallo, D. Tranchida and A. J. Müller, Effect of compatibilizer addition on the surface nucleation of dispersed polyethylene droplets in a self-nucleated polypropylene matrix, *Polymer*, 2022, **263**, 125511.

25 W. Huang, Y. Zhang, B. Chen, H. Yang, K. Shen, X. Gao and Q. Fu, The effect of annealing time on morphology, mechanical properties, and thermal conductivity of HDPE pipes produced by rotational shear, *Mater. Today Commun.*, 2022, **31**, 103321.

26 M. Liu, Y. Wang, J. Chen, J. Luo, Q. Fu and J. Zhang, The retarded recovery of disentangled state by blending HDPE with ultra-high molecular weight polyethylene, *Polymer*, 2022, **192**, 122329.

27 M. F. Diop, W. R. Burghardt and J. M. Torkelson, Well-mixed blends of HDPE and ultrahigh molecular weight polyethylene with major improvements in impact strength achieved via solid-state shear pulverization, *Polymer*, 2014, **55**, 4948.

28 Y. Sui, Z. J. Qiu, Y. Liu, J. C. Li, Y. Cui, P. Wei and Q. Zhou, Ultra-high molecular weight polyethylene (UHMWPE)/high-density polyethylene (HDPE) blends with outstanding mechanical properties, wear resistance, and processability, *J. Polym. Res.*, 2023, **30**, 222.

29 H. Yang, G. Yilmaz, J. Jiang, J. Xie, T. Langstraat, R. Chu, M. van Es, P. Garg and L.-S. Turng, Pelletizing ultra-high molecular weight polyethylene (UHMWPE) powders with a novel tapered die and addition of high density polyethylene (HDPE): Processing, morphology, and properties, *Polymer*, 2022, **256**, 125171.

30 H. Shen, L. He, C. Fan, B. Xie, W. Yang and M. Yang, Improving the integration of HDPE/UHMWPE blends by high temperature melting and subsequent shear, *Mater. Lett.*, 2015, **138**, 247.

31 Q. Zhang, L. Lan, Z. Zheng, P. Liu, H. Wu, S. Guo, C. Lin and G. He, Constructing highly oriented and condensed shish-kebab crystalline structure of HDPE/UHMWPE blends via intense stretching process: Achieving high mechanical properties and in-plane thermal conductivity, *Polymer*, 2022, **241**, 124532.

32 A. B. Boscoletto, R. Franco, M. Scapin and M. Tavan, An investigation on rheological and impact behaviour of high density and ultra high molecular weight polyethylene mixtures, *Eur. Polym. J.*, 1997, **33**, 97.
33 P. Gennes, Scaling Concept In Polymer Physics, *Phys. Today*, 1979, **6**, 51.
34 M. Doi and S. F. Edwards, *Theory of Polymer Dynamics*, New edn, 1986.
35 S. Rastogi, D. R. Lippits, G. W. M. Peters, R. Graf, Y. Yao and H. W. Spiess, Heterogeneity in polymer melts from melting of polymer crystals, *Nat. Mater.*, 2005, **4**, 635.
36 M. Avrami, Kinetics of Phase Change. I General Theory, *J. Chem. Phys.*, 1939, **7**, 1103.
37 K. Harnisch and H. Muschik, Determination of the Avrami exponent of partially crystallized polymers by DSC (DTA) analyses, *Colloid Polym. Sci.*, 1983, **261**, 908.
38 Q. Jiasheng and H. Pingsheng, Non-isothermal crystallization of HDPE/nano-SiO_2 composite, *J. Mater. Sci.*, 2003, **38**, 2299.
39 T. Ozawa, Kinetics of non-isothermal crystallization, *Polymer*, 1971, **12**, 150.
40 A. Dobreva and I. Gutzow, Activity of substrates in the catalyzed nucleation of glass-forming melts. II. Experimental evidence, *J. Non-Cryst. Solids*, 1993, **162**, 13.
41 H. L. Friedman, Kinetics of thermal degradation of char-forming plastics from thermogravimetry. Application to a phenolic plastic, *J. Polym. Sci., Part C: Polym. Symp.*, 1964, **6**, 183.